O Binding Sites on Stepped Pt(111) Surfaces

Peter J. Feibelman,[1] Stefanie Esch,[2] and Thomas Michely[2]

[1]*Sandia National Laboratories, Albuquerque, New Mexico 87185-1413*
[2]*Institut für Grenzflächen und Vakuumphysik, Forschungszentrum Jülich GmbH, D-52425, Jülich, Germany*
(Received 13 May 1996; revised manuscript received 31 July 1996)

First-principles calculations show that O adatoms are attracted to step edges on Pt(111), gaining 0.2 to 0.3 eV per nearest neighbor step-edge Pt atom, and that they favor "fcc-like" over "hcp-like" sites by ~ 0.4 eV. These preferences account for the different appearances, in scanning tunneling micrographs, of O-saturated, *A*- and *B*-type island edges on Pt(111). They imply that O binds in a three-fold, fcc hollow site behind a *B* step, while twofold edge bridging is favored for *A* steps. [S0031-9007(96)01151-9]

PACS numbers: 68.35.Bs

In this Letter, we compare scanning tunneling micrographs and local density approximation (LDA) calculations [1] of O-saturated, monatomic-height steps on Pt(111). Representative micrographs, such as that of Fig. 1, are of markedly different appearance near the two close-packed step types that exist on this surface. The calculations yield a simple interpretation of the difference in terms of energetic preferences for "twofold, overedge," and "threefold, overterrace" O binding geometries at so-called *A* and *B* steps, whose "risers" are, respectively, (100) and (111) microfacets (cf. Fig. 2).

The behavior of gas fragments near defects on transition metal surfaces is central to scientific issues from the interpretation of scanning tunneling micrographs (STM) [2] to the energetics of reconstructive phase transitions [3]. The way that light adspecies interact with surface defects is also the key to important technological questions, including the mechanisms and performance of "surfactant" species in promoting layer-by-layer crystal growth [4], and the nature of heterogeneous catalytic reactions [5]. On surfaces vicinal to Pt(111), O is known to prefer binding to steps [6,7]. Preadsorbed O has been shown to promote layer-by-layer growth of Pt(111) [4], and at higher temperatures, ad-O causes a "step-doubling" reconstruction [3]. Thus the O/Pt system exhibits many of the phenomena one would like to understand.

On the low-Miller-index surfaces of metals, adatoms typically bind in the highest coordination site available. Thus it is not surprising that in the saturation $p(2 \times 2)$-O/Pt(111) structure [6], O atoms occupy fcc threefold hollows [8]. On a stepped surface, O binding need not be optimal at the highest coordination site, because the O adatoms' demands must now be balanced against those of the various, geometrically inequivalent Pt atoms.

Figure 1 shows that O adatoms prefer steps to terraces on islanded Pt(111); essentially all the island edges in the micrograph exhibit nearby O-induced features, while the terraces are relatively free of O. This evidence that passivating low coordination atoms at island edges dominates the choice of binding site is not unexpected. What is remarkable is how differently the

O adatoms affect the appearances of (100) and (111) microfacets.

In what follows we interpret this difference via LDA total energy calculations. The LDA's qualitative predictions are likely to be trustworthy, since structural energy differences are rather large for O adsorption on Pt. By showing that the different appearances of the O-covered steps relate simply to theoretical O binding geometries, we hope to establish O/Pt as a standard reference system for developing our understanding of gas interactions with defects on transition metals.

Our micrographs were obtained in a UHV-STM apparatus [9]. Prior to each adsorption experiment, the Pt(111) crystal was cleaned until no trace of impurities was detectable in STM topographs or Auger spectra, using cycles of Ar^+ ion bombardment, then exposure to 5×10^{-6} mbar of O_2 at 750 K and annealing to 1300 K. We create the saturation $p(2 \times 2)$-O structure while cooling down from the last anneal by exposing the Pt(111) surface 2×10^{-5} mbar O_2, starting at 500 K. Throughout the range of applied tunneling voltages (± 600 mV) and currents (≤ 15 nA), oxygen images as a depression on the terraces. To obtain a surface with a large number of both types of close-packed step edges covered by O, we
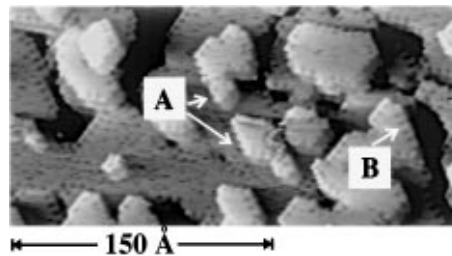

FIG. 1. Scanning tunneling micrograph of O-covered islands on Pt(111), created by deposition of Pt onto the O-$p(2 \times 2)$ structure at 300 K. Along the close-packed step edges that bound the islands, adsorbed O gives rise to a (2×1) periodic structure. At the *B* steps, O forms dark depressions on the upper terrace. At *A* steps, O creates a scalloped appearance. The topographs are differentiated to enhance contrast, with illumination from the left.

deposit several monolayers of Pt onto the O-covered surface, by sublimation of a heated Pt foil. This deposition results in partial loss of oxygen from the terraces, while the step edges remain O decorated.

Figure 1 shows O-covered step edges after Pt deposition at 300 K Near B steps, O forms a 2×1 row of dark dots along the upper step edge. Since oxygen images as a depression with the same corrugation for both the occasionally observable $p(2 \times 2)$ patches on the terrace and the (2×1) rows along the B steps, we conclude that it is adsorbed *on* the upper edge of the step (i.e., it is not incorporated in the surface layer). According to the registry with the $p(2 \times 2)$ patches on the terrace, since $p(2 \times 2)$-O occupies fcc hollows on Pt(111) [8], the O resides in fcc hollow sites behind each B step.

O also gives rise to 2×1 periodic images along A steps, but with a markedly different appearance, scalloped rather than straight step edges, and no dark dots. Although we cannot say from the STM image just where the O adatoms lie, it is clear that they sit closer to the step edges than for B steps.

Because O and Pt are strong pseudopotential atoms, and because vicinal surface calculations involve substantial numbers of atoms in the unit cell, it is convenient to use QUEST, a parallel, linear combination of atomic orbitals (LCAO) implementation of the LDA [10], to obtain theoretical, O binding energies. We use Hamann [11] and Troullier-Martins (TM) pseudopotentials [12] to represent electron interactions with Pt and O nuclei (the TM O pseudo-wave-functions' relative smoothness allows for coarser coordinate-space meshes [13]), and the Ceperley-Alder potential to account for exchange and correlation [14]. Basis sets for the vicinal Pt slabs are as in Ref. [15]. In addition, we center two s-, two p-, and one d-like orbital [16] at each O site.

To obtain O heats of adsorption, we compare the energies of geometrically relaxed, clean and O-covered, periodic vicinal slabs. The slabs are at least seven (111) layers thick [17] and their terraces three to five atomic rows wide. To perform a slab-geometry optimization, we fix several [17] central Pt layers at bulk-Pt separations and relax the rest, plus any O atoms, via Johnson's iteration scheme [18]. O atoms are initially placed near symmetry sites, and, as Table I shows, they remain rather symmetrically bonded, with three bonds ~ 2.0 Å long on terraces, or two that are ~ 1.9 Å long, at edge bridges. To obtain meaningful energies, we allow the same set of Pt atoms to move, for each slab, both when the slab is clean and when it is O covered. We check that the forces on the central layers are small; they would be zero for asymptotically thick slabs. We place adatoms symmetrically on both sides of each slab to speed convergence to electronic self-consistency. We sample surface brillouin zones with equally spaced k vectors, separated by no more than 0.2 bohr^{-1}.

On Pt(111), O adsorption saturates at 0.25 monolayer coverage [6]. LEED analysis implies that, at that coverage,

O atoms reside in every other fcc threefold hollow, in an ordered $p(2 \times 2)$ arrangement. The first and second Pt layers are somewhat buckled in the presence of the adatoms, and the O-Pt bond length is 2.02 Å [8]. In good agreement, we obtain an O-Pt bond length of 2.00 Å for the midterrace fcc site on Pt(221) [above "*tf*" in Fig. 2(b)].

Because it is not *a priori* clear that 1×1 O-adsorption geometries are unfavorable on vicinal surfaces, even though they are on (111) terraces, we compare 1×1 and 2×1 O adsorption on Pt(211). The results are that, when O bridges step-edge atoms, its binding energy is 0.48 eV/adatom higher when every other bridge site is occupied, in a 2×1 structure, than when every bridge site is filled. The same comparison, for fcc sites on the terrace above and adjacent to a step, yields an advantage for the lower coverage structure of 0.19 eV. These results imply, as can be expected for an atom that binds as ionically as O does, that occupying nearest neighbor sites is unfavorable both near steps and on terraces [19]. Confirmation that step saturation corresponds to occupation of every other near-step adsorption site is evident in Fig. 1. In this representative micrograph, the O-related features at both step types have a periodicity of twice the Pt-Pt spacing along the steps. We therefore restrict further attention to 2×1 adsorption geometries.

The LDA results for 2×1 O adsorption, presented in Table I, unambiguously predict that, in an STM image of an A step, O adatoms should show up right at the step edge, while at a B step, the O effect should appear on the upper terrace, behind the step edge, *just as we see in Fig. 1.* At A steps, where the STM images show scalloped edges, the LDA results favor the edge bridge by >0.3 eV over the near-edge fcc site [20], while we find no energy minimum in the near-edge, hcp neighborhood. At B steps, where the STM images show dark dots over the upper terrace, it is the fcc hollows closest to the step tops that are preferred, by 0.22 eV relative to the edge-bridging geometry, by 0.55 eV relative to the near-edge hcp site, by 0.38 eV relative to the midterrace fcc hollow, and by 0.70 eV relative to the fcc site at the step bottom.

Apart from their apparent agreement with experiment, the results in Table I are compelling because they obey, and can be interpreted via two simple, physically meaningful rules. The rules are as follows:

(1) Bonding in fcc sites is preferred to hcp by ~ 0.4 eV. In saying this, we mean the concept of "fcc site" to include edge bridging at an A step, where [cf. Fig. 2(a)] there is no Pt atom directly below the O adatom on the lower terrace in front of the step. Similarly, the idea of hcp binding is extended to edge bridging at a B step [i.e., binding at "*eb*" in Fig. 2(b)], where there is a Pt atom on the lower terrace in front of the step, below the ad-O.

(2) An O adatom gains binding energy in rough proportion to the number of its nearest neighbors that are step-edge atoms. The gain is ~ 0.25 eV if the O atom has only one step-edge neighbor, it is ~ 0.4 eV if the O atom's nearest neighbors are one terrace and two step-edge atoms,

TABLE I. LDA binding energies, E_B (eV), and distances to nearest neighbors, computed for (2×1) superlattices of O adatoms in various sites [cf. Figs. 2(a) and 2(b)], on various slabs whose surfaces are vicinal to Pt(111). The LDA reference energy for isolated O includes a spin-polarization contribution of 0.69 eV. Binding energies in the "estimated E_B (eV)" column follow from the two rules given in the main text, starting from the LDA value of 5.28 eV for the *tf* site on Pt(221).

Site description	Vicinal surface	Figure; label	Step type	Dist.'s (in Å) to near neighbors	LDA E_B (eV)	Estimated E_B (eV)
Edge bridge	(211)	2(a); filled dots	A	1.90, 1.90	5.85	5.88
Near-edge fcc	(211)	2(a); *ef*	A	2.02, 2.00, 2.00	5.51	5.53
Near-edge hcp	(211)	2(a); *eh*	A		—[a]	5.28
Edge-bridge	(322)		A	1.90, 1.90	5.87	5.88
Near-edge fcc	(322)		A	2.03, 2.01, 2.01	5.57	5.53
Step-bottom fcc	(322)		A	2.00,[b] 2.00,[b] 1.98	5.10	—[c]
Edge bridge	(221)	2(b); *eb*	B	1.90, 1.90	5.44	5.48
Midterrace fcc	(221)	2(b); *tf*	B	2.00, 2.00, 2.00	5.28	5.28
Midterrace hcp	(221)	2(b); *th*	B	1.99, 2.01, 2.01	4.90	4.88
Near-edge fcc	(221)	2(b); filled dots	B	1.99, 1.99, 2.03	5.66	5.68
Near-edge hcp	(221)	2(b); *eh*	B	2.00, 2.02, 2.02	5.11	5.13
Step-bottom fcc	(221)	2(b); *bf*	B	1.99,[d] 1.99,[d] 2.04	4.96	—[c]

[a]No local minimum could be found in this vicinity.

[b]Distances to adjacent step-bottom atoms; nearest step-edge atoms are 2.90 Å away.

[c]See Ref. [21].

[d]Distances to nearby bottom-terrace atoms; nearest step-edge atoms are 3.17 Å away.

and it is $\sim$0.6 eV if the ad-O hangs off the step edge, coordinated only to two step-edge Pt atoms [21].

Rule (1) represents the needs of the O adatoms; it says that they prefer fcc binding sites on vicinal surfaces, just as they do on Pt(111) [8]. Rule (2) represents the dominant demand of the substrate, that its least-coordinated atoms be passivated first [6,7]. Step-edge atoms, on both *A* and *B* steps, have 7 neighbors, compared to 9 for terrace atoms and 10 or 11 for step-bottom atoms [22]. Thus, the total energy of the system is lowered most when O adatoms abate the edge Pt atoms need for neighbors. In addition, per-edge-atom passivation is better when adatoms are *only* bonded to step-edge neighbors or when the passivating O atom has only one edge neighbor.

These rules yield simple interpretations of the structures seen in Fig. 1: (I) At *A* steps, the edge bridge is preferred to the adjacent threefold, overterrace site [above the label "*eh*" in Fig. 2(a)], which also allows for passivation of two step-edge Pt atoms, because an *eh* site is an hcp hollow. Its occupation, according to rule (1), incurs an energetic penalty of 0.4 eV relative to binding in an fcc-like site. The edge-bridging site is a quasi-fcc hollow. It is not a threefold site, of course, since there is a step present and a Pt neighbor is thus missing. But, as the 0.43 eV difference in the binding energies for edge bridging at *A*- and *B*-type steps shows (cf. Table I), removing rows of atoms to create a step does little to affect the fcc-hcp structural energy difference [23].

There is a fcc hollow at an A step that allows an O adatom to have one Pt edge neighbor [labeled "*ef*" in Fig. 2(a)]. But it only provides the $\sim$0.25 eV advantage of passivating *one* step edge Pt, plus the fcc hollow advantage

of 0.4 eV. In the edge-bridging site, the O passivates *two* edge neighbors and is in a quasi-fcc site. The extra binding accrued by passivating two edge Pt atoms is decisive and makes the edge-bridging site optimal.

(II) At *B* steps, an O adatom prefers the threefold, overterrace site because it is an fcc hollow, adjacent to two step-edge Pt atoms, accruing a passivation energy gain of 0.4 eV. This 0.2 eV better than the quasi-hcp edge bridge ["*eb*" in Fig. 2(b)], where a 0.6 eV passivation-energy gain is counteracted by a $\sim$0.4 eV hcp penalty.

The remarkable correspondence between predicted O-binding preferences and STM images invites further study of O adsorption on Pt. (1) For example, our large computed energy differences, *amounting to as much as 0.4 eV for structures that differ only in the locations of second neighbor atoms,* suggest O/Pt(111) as a venue for determining the (elusive) source of fcc-hcp binding energy differences on close-packed terraces [23]. (2) Twofold vs threefold O coordination at the two step types could be confirmed via vibration measurements. (3) Success in describing O at monatomic-height steps suggests continuing by exploring the energetics of the O-induced step-doubling transition [3].

(4) Finally, to extract full value from Fig. 1, we should learn why our dark spots are dark, how far behind the *B*-step edges they should be, and also where the O's sit in the scalloped, *A*-edge images. We have performed local density of states (LDOS) calculations for this purpose [24], finding relative minima of the Fermi-level LDOS above threefold bonded O adatoms at *B* steps; this supports the idea that the dark spots in Fig. 1 mark the ad-O locations. In surprising contrast, LDOS *maxima,* not
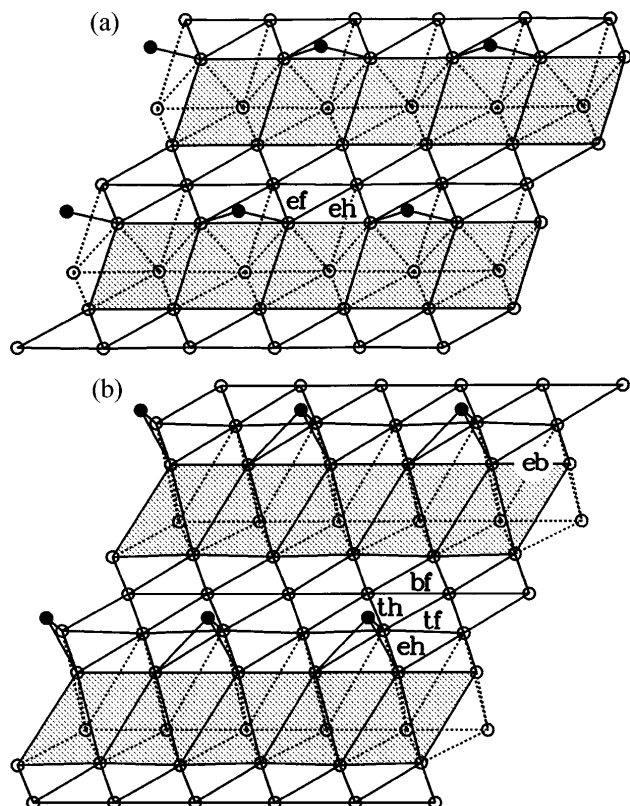
FIG. 2.   Schematics of an O-saturated *A* step (a) and a *B* step (b). In each case, the O atoms (filled circles) and the Pt atoms (open circles) are located in their optimal binding sites. The site labels in the two panels correspond to the same labels in Table I.

minima, lie above O's adsorbed at *A* steps. Thus, in the scalloped, *A*-step images, the bright protuberances, not the dark indentations, mark the adatom sites. Apparently, more ionic bonding at edge bridges is mediated by partial occupation of high-lying O *p* states. This gives rise to LDOS maxima which are absent when O binds more covalently, as it does on terraces.

[1] See *The Theory of the Inhomogeneous Electron Gas*, edited by S. Lundqvist and N. H. March (Plenum Press, New York, 1983); also, W. E. Pickett, Comp. Phys. Rep. **9**, 115 (1989).

[2] See, e.g., P. Sautet, J. C. Dunphy, D. F. Ogletree, C. Joachim, and M. Salmeron, Surf. Sci. **315**, 127 (1994).

[3] E. Hahn, H. Schief, V. Marsico, A. Fricke, and K. Kern, Phys. Rev. Lett. **72**, 3378 (1994), and references therein.

[4] S. Esch, M. Hohage, T. Michely, and G. Comsa, Phys. Rev. Lett. **27**, 518 (1994).

[5] See, e.g., J. Xu and J. T. Yates, Jr., J. Chem. Phys. **99**, 725 (1993).

[6] J. L. Gland and V. N. Krochak, Surf. Sci. **75**, 733 (1978).

[7] H. Wang, R. G. Tobin, G. B. Fisher, C. L. DiMaggio, and D. L. Lambert, Surf. Sci. (to be published).

[8] N. Materer, U. Starke, A. Barbieri, R. Doll, K. Heinz, M. A. Van Hove, and G. A. Somorjai, Surf. Sci. **325**, 207 (1995). An "fcc hollow" is a threefold site with no Pt atom directly below the O, in the first subsurface layer.

[9] Th. Michely, Forschungszentrum Jülich Report No. Jül-Bericht 2569 (to be published).

[10] M. P. Sears, P. A. Schultz, and P. J. Feibelman (to be published).

[11] D. R. Hamann, Phys. Rev. B **40**, 2980 (1989).

[12] N. Troullier and J. L. Martins, Phys. Rev. B **43**, 1993 (1991).

[13] The "coarse" mesh has a spatial interval of 0.26 bohr.

[14] D. M. Ceperley and B. J. Alder, Phys. Rev. Lett. **45**, 566 (1980), as parametrized by J. Perdew and A. Zunger, Phys. Rev. B **23**, 5048 (1981).

[15] P. J. Feibelman, Phys. Rev. B **52**, 16 845 (1995).

[16] Their radial parts are Gaussian contractions, $R_l(r) = r^l \sum_\alpha c_\alpha \exp(-\alpha^2)$, with $\{\alpha\} = \{0.1500, 0.4921, 1.8533, 2.4117\}$ and $\{0.1500\}$, for $l = 0$, $\{\alpha\} = \{0.1400, 0.4453, 1.2521, 3.8450\}$ and $\{0.1400\}$, for $l = 1$, and $\{\alpha\} = 0.65$, for $l = 2$. The c_α's in the four-α contractions are fixed via fits to numerical wave functions for isolated, neutral O.

[17] For Pt (211) we use a 27-layer slab, fixing the central 3 layers at bulk Pt separations. For Pt (221) and (322), we use 29 and 45 Pt layers, in both cases fixing the central 5.

[18] D. D. Johnson, Phys. Rev. B **38**, 12 807 (1988).

[19] There must be a strong covalent component to the bonding of O near step edges on Pt (211): The dipoles associated with O in edge-bridging sties shift the Pt (211) work function by roughly 0.6 eV/adatom, compared to about 0.15 eV/adatom in the near-edge, fcc site. Thus extra dipole-dipole repulsion in the edge-bridging site must be exceeded by the benefit of passivating two Pt edge atoms.

[20] That the computed binding energies on Pt (211) and Pt (322) are close indicates rapid convergence with terrace width. Of course, the Pt (322) results represent isolated *A* steps better, since its steps are twice as far apart.

[21] Extra "rules" are needed for step bottom adsorption. Note, in Table I, that the energetic penalty per bottom neighbor is considerably bigger at a *B* than at an *A* step.

[22] 10 for *A* or 11 for *B* steps.

[23] The preference for fcc sites on flat Pt (111) presumably reflects the projection into fcc hollows of nonbonding orbitals corresponding to the Pt bands near the Fermi level. That this projection persists near steps is not so surprising, since it underlies Pt's growth as an fcc crystal.

[24] A complete account of these results is in preparation [P. J. Feibelman (unpublished)].